Published in final edited form as:
Hear Res. 2014 August ; 314: 20–32. doi:10.1016/j.heares.2014.05.001.

Localization of kainate receptors in inner and outer hair cell synapses

Taro Fujikawa[a,b], **Ronald S. Petralia**[c], **Tracy S. Fitzgerald**[d], **Ya-Xian Wang**[c], **Bryan Millis**[a], **José Andrés Morgado-Díaz**[e], **Ken Kitamura**[b], and **Bechara Kachar**[a]

[a]Laboratory of Cell Structure and Dynamics, National Institute on Deafness and Other Communication Disorders, National Institutes of Health, Bethesda, MD 20892, USA

[b]Department of Otolaryngology, Tokyo Medical and Dental University, Bunkyo-ku, 113-8519, Tokyo, Japan

[c]Advanced Imaging Core, National Institute on Deafness and Other Communication Disorders, National Institutes of Health, Bethesda, MD 20892, USA

[d]Mouse Auditory Testing Core Facility, National Institute on Deafness and Other Communication Disorders, National Institutes of Health, Bethesda, MD 20892, USA

[e]Cellular Biology Division, National Cancer Institute, Rio de Janeiro, Brazil, CEP 20230-050

Abstract

Glutamate plays a role in hair cell afferent transmission, but the receptors that mediate neurotransmission between outer hair cells (OHCs) and type II ganglion neurons are not well defined. A previous study using *in situ* hybridization showed that several kainate-type glutamate receptor (KAR) subunits are expressed in cochlear ganglion neurons. To determine whether KARs are expressed in hair cell synapses, we performed X-gal staining on mice expressing *lacZ* driven by the *GluK5* promoter, and immunolabeling of glutamate receptors in whole-mount mammalian cochleae. X-gal staining revealed GluK5 expression in both type I and type II ganglion neurons and OHCs in adults. OHCs showed X-gal reactivity throughout maturation from postnatal day 4 (P4) to 1.5 months. Immunoreactivity for GluK5 in IHC afferent synapses appeared to be postsynaptic, similar to GluA2 (GluR2; AMPA-type glutamate receptor (AMPAR) subunit), while GluK2 may be on both sides of the synapses. In OHC afferent synapses, immunoreactivity for GluK2 and GluK5 was found, although GluK2 was only in those synapses bearing ribbons. GluA2 was not detected in adult OHC afferent synapses. Interestingly, GluK1, GluK2 and GluK5 were also detected in OHC efferent synapses, forming several active zones in each synaptic area. At P8, GluA2 and all KAR subunits except GluK4 were detected in OHC afferent synapses in the apical turn, and GluA2, GluK1, GluK3 decreased dramatically in the basal turn. These results indicate that AMPARs and KARs (GluK2/GluK5) are localized to IHC afferent synapses, while only

Corresponding authors: Ronald S. Petralia, 50 South Drive, 50/4142, NIDCD/NIH, Bethesda, MD 20892-8027, petralia@nidcd.nih.gov, 301-496-3804.

KARs (GluK2/GluK5) are localized to OHC afferent synapses in adults. Glutamate spillover near OHCs may act on KARs in OHC efferent terminals to modulate transmission of acoustic information and OHC electromotility.

Keywords

Hair cell; Afferent; Efferent; Synapse; Glutamate receptor; Cochlea; AMPA receptor; Kainate receptor

1. Introduction

Hearing requires both the transduction of sounds into electrical impulses by cochlear hair cells and the relaying and processing of that information along a cascade of neurons (nerve cells) in the brain via chemical synapses between them. Defects in any of these processes can lead to hearing loss. The first synapses in this sequence link the sound-transducing hair cells with the processes of the primary neurons, called spiral ganglion cells, which relay information to the brainstem. Synaptic transmission between the hair cell and the ganglion cell processes depends on release of a chemical neurotransmitter, mainly glutamate, and its binding to neurotransmitter receptor molecules.

About 95% of auditory afferent neurons are type I ganglion neurons (Spoendlin, 1969). Each type I neuron sends a peripheral projection to an inner hair cell (IHC), forming a ribbon synapse (Liberman, 1980; Liberman, 1982; Moser et al., 2006; Safieddine et al., 2012), where the presynaptic neurotransmitter glutamate and postsynaptic AMPA (<alpha>-amino-3-hydroxy-5-methyl-isoxazolepropionic acid)-type glutamate receptors (AMPARs) mediate excitatory transmission (Matsubara et al., 1996; Ruel, et al., 1999; Glowatzki and Fuchs, 2002). Multivesicular release at this synapse achieves frequent excitatory postsynaptic currents (EPSCs) in type I afferent neurons and causes continuous and rapid transmission of acoustic information. Type II neurons constitute the remaining 5 percent of afferent neurons. Each type II neuron forms a thin, unmyelinated dendrite contacting many outer hair cells (OHCs). Each OHC has 3 to afferent terminals (Liberman et al., 1990) and some of them do not bear a ribbon synapse (Hashimoto and Kimura, 1988; Liberman et al., 1990; Huang et al, 2012). OHC/type II afferent transmission is also glutamatergic, but EPSCs in type II neurons are much smaller in frequency and amplitude, and significantly slower in kinetics compared to averaged EPSCs recorded in type I neurons (Weisz et al., 2009), so that summated stimulation is required to produce an action potential in type II afferent neurons (Weisz et al., 2012). The specific receptor involved remains unknown, because there is no immunoreactivity for AMPARs in type II afferent nerve terminals (Matsubara et al., 1996; Liberman et al., 2011).

OHCs also are innervated by myelinated fibers from the medial olivocochlear (MOC) efferent projections, forming several synapses at the base (Liberman and Brown, 1986). The MOC system is cholinergic and suppresses the electromotile response of OHCs (Wersinger and Fuchs, 2011; Elgoyhen and Katz, 2012), providing a feedback system to optimize cochlear amplification (LePage, 1989). Acetylcholine (ACh) is the only well-defined neurotransmitter in OHC efferent synapses, but additional molecules are proposed to be

involved in the transmission as neuromodulators, including gamma amino butyric acid (GABA). It is suggested that GABAergic signaling contributes to the long-term maintenance of hair cells or normal OHC electromotility (Maison et al., 2006; Maison et al., 2009). Furthermore, a recent study shows that released GABA acts on presynaptic $GABA_B$ receptors expressed in OHC efferent terminals to downregulate the release of ACh (Wedemeyer, et al., 2013).

Ionotropic glutamate receptors (GluRs) include three major families; NMDA-type, AMPA-type and kainate-type receptors (KARs). GluRs mediate neurotransmission at excitatory synapses, but neuronal KAR-mediated EPSCs have distinct physiological feature of smaller amplitude and slower deactivation kinetics, compared to AMPA-mediated EPSCs and are shaped by auxiliary KAR subunits, such as tolloid-like (NETO1) and NETO2 proteins (Lerma and Marques, 2013). In addition, presynaptic KARs can act as neuromodulators of synapse transmission to control transmitter release in a bidirectional manner; frequency-dependent facilitation and depression of transmitter release via presynaptic KARs is demonstrated at mossy fiber synapses in the hippocampus (Lerma, 2003) and at parallel fiber synapses in the cerebellar cortex (Delaney and Jahr, 2002). Moreover, postsynaptic KARs are thought to regulate neuronal excitability both through slowly deactivated ionotropic KARs and through G protein-coupled metabotropic KARs (Lerma and Marques, 2013).

A previous study using *in situ* hybridization showed that several KAR subunits (GluK1, GluK2, GluK4, GluK5) are expressed in cochlear ganglion neurons (Niedzielski & Wenthold, 1995). Another study reported that KARs are expressed in IHC afferent synapses and suggested that KARs contribute to hair cell acoustic transmission, based on physiological data using a GluK1-specific antagonist (Peppi et al., 2012). These findings suggest that KARs are involved in normal cochlear function for synaptic transmission or modulation. In order to determine whether KARs are expressed in synapses of IHCs and OHCs, we performed immunolabeling of all the subtypes of KARs in the adult mammalian cochlea. We also performed auditory testing on mice that lacked GluK5. We found that KARs (GluK2/GluK5) are the main postsynaptic GluRs in OHC afferent synapses and that the expression pattern of KARs show developmental changes. Interestingly, KARs are also expressed in OHC efferent terminals. Moreover, we detected both pre- and postsynaptic KARs in IHC afferent synapses.

2. Materials and Methods

2.1. Animals

GluK5 knockout mice (GluK5 KO; strain B6. 129P2-*Grik5*^{tm1Dgen}/J), was obtained from the Jackson Laboratories (generated by Deltagen). This strain has been backcrossed to C57BL/6 mice and has a targeted deletion inside the GluK5 (*Grik5*) gene (from base 1936 to base 2006) that is replaced with a reporter gene, *lacZ*. We confirmed that X-gal staining in brain sections of the mice (data not shown) is consistent with previous studies of GluK5 cellular distribution in the brain (Darstein, et al., 2003). All the animals used in this study were euthanized in accordance with National Institutes of Health (NIH) guidelines.

2.2. X-gal staining of cochleae

Cochleae from GluK5 KO mice were fixed in 4% paraformaldehyde with 0.02% Nonidet P-40 in phosphate buffered saline (PBS) for ~ 1 hour at 4°C. Cochleae were decalcified in 5% EDTA for three days at 4°C, washed in rinse buffer (0.01% sodium deoxycholate, 0.02% Nonidet P-40, 2 mM magnesium chloride in PBS) for 1 hour and stained in 1 mg/ml X-gal/5 mM potassium ferrocyanide/5 mM potassium ferricyanide in rinse buffer overnight at 37°C (Bianchi, et al., 2002; Corradi, et al., 2003). Cochleae were dissected for whole-mount preparation or processed further for sections; Cochleae were cryoprotected in 20% sucrose overnight at 4°C before embedding in Tissue-Tek O.C.T. compound (Sakura) using a vacuum to remove bubbles inside, and cut at 16 μm thickness on a Leica Cryostat (OT -15°C, CT -15°C). After pos t-fixation with 4% paraformaldehyde for 10 min, sections were incubated in BLOXALL (Vector Laboratories), blocked in 5% bovine serum albumin (BSA) and incubated in mouse anti-neurofilament-H (clone RT97; Sigma-Aldrich, 1:1000) overnight at 4°C. Sections were then incubated in HRP-conjugated secondary antibody (Santa Cruz Biotechnology, 1:500) and DAB stain was developed with ImmPACT DAB (Vector Laboratories).

2.3. Whole-mount immunofluorescence

Temporal bones of Sprague-Dawley rats (4-6 weeks old or postnatal day (P) 8) were quickly removed and fixed in 2% paraformaldehyde for 10 min at room temperature, if not otherwise specified (Grati, et al., 2012). Cochlear tissues were then dissected, permeabilized with 0.5% Triton X-100 for 30 min and blocked with 5% bovine serum albumin. Primary antibody was incubated as described below. Synaptic markers were also used; ribeye (Synaptic Systems, 1:200), CtBP2 (clone 16/CtBP2; BD Biosciences, 1:200), PSD-93 (Alomone labs, 1:200), PSD-93 (clone N18/30 and clone N18/28; NeuroMab, 1:200), VAMP2 (clone 69.1; Synaptic Systems, 1:200), Na^+/K^+-ATPase α3 (Santa Cruz Biotechnology, 1:50), synapsin (Millipore, 1:500). The tissue then was incubated in Alexa Fluor 488- and 568-conjugated secondary antibodies and Alexa Fluor 674 phalloidin (Molecular Probes) and then fixed again by immersion in 4% paraformaldehyde for ~15 min before mounting using Prolong Anti-fade reagent (Invitrogen). Confocal images were acquired using a Nikon TE-2000 inverted microscope outfitted with a CSU-21 Yokogawa spinning disk (Perkin-Elmer), Plan Apo 100×/1.40 NA objective, and Hamamatsu Orca-ER CCD. Image acquisition, including stacks, was managed through Volocity imaging software (Perkin-Elmer). All image analyses, including fluorescence intensity quantification, peak distance measurement, maximum intensity projection, and 3D reconstruction, were performed with NIS-Elements software (Nikon Instruments, Inc.). For each immunofluorescence labeling and quantification experiment in Fig. 6, we used at least three cochleae from at least two (and typically three or more) rats from different tissue preparations. Control sections, lacking the primary antibodies, were run in most experiments and none of the specific labeling described here for all antibodies was shown.

Peak distance measurement was performed according to the following procedure: all the samples shown in Fig. 3 and Fig. 4 were prepared using the same method used for GluA2 labeling, as described in section 2.4 below. At least three cochleae from at least two (and typically three or more) rats from different tissue preparations were used for each distance

measurement. Subsequent to confocal image stack acquisition from the cochlear basal turn, all IHC's within a given stack (average of 10 IHC's/frame) were visually scanned to select apical- or lateral- view synapses. Fluorescence intensity and peak distance were measured for each synapse along a line transecting the center of the double-immunofluorescence pattern (based on their relative orientation with each other), using NIS-Elements (method illustrated in Fig. 3).

2.4. Glutamate receptor immunoreactivity

Immunoreactivity of KARs was based on methods used previously (Meyer, et al., 2009; Liberman, et al., 2011). Cochlear tissue was labeled with GluK1 (Alomone, 1:200), GluK2 (Alomone, 1:200), GluK3 (Synaptic Systems, 1:200) and GluK5 (Synaptic Systems, 1:400) in PBS overnight at 4°C. All 4 anti bodies were used previously in a study of the brain (Marrocco et al, 2012). GluK1 and GluK2 are affinity-purified rabbit polyclonal antibodies; the immunogen was a peptide corresponding to amino acids 402-417 (N-terminus) or 858-870 (C-terminus) of rat GluK1 or GluK2, respectively. GluK1 and GluK2 antibodies show immunoreactivity in rats (GluK2 also shows immunoreactivity in mice). GluK1 produces a clean western blot with three bands using brain membranes of rat; bands are absent after preincubation with the control peptide; in contrast, GluK2 antibody produces a clean western blot with only a single band of the predicted size, using brain membranes of rat (Alomone data). GluK3 and GluK5 are affinity-purified rabbit polyclonal antibodies; the immunogen was a recombinant protein of amino acids 845-919 or 828-979 (C-terminus) of rat GluK3 or GluK5, respectively. GluK3 antibody produces a clean western blot with a single, wide band around the predicted size, using the synaptosomal fraction (P2) of rat; in contrast, GluK5 antibody produces a clean western blot with a single band of the predicted size, using the synaptic membrane fraction (LP1) of rat (Synaptic Systems data). Both antibodies from Synaptic Systems show reactivity in rats and mice and are specific for their respective subunits.

For GluK4 labeling, we tried all possible protocols (paraformaldehyde or methanol for fixative, different temperatures and times for fixation, heat-mediated or microwave-mediated antigen retrieval for labeling) using a commercially available antibody (Abcam, ab10101). This antibody is a rabbit polyclonal (protein A purified) made from a synthetic peptide (amino acids 60-73 of human KA1) conjugated to keyhole limpet hemocyanin. It detects a band of the predicted size on western blots (Abcam datasheet). However, we could not achieve clear immunoreactivity for GluK4 in rat cochleae from P8 to 6 weeks of age.

For GluA2 (clone 6C4; Chemicon, 1:200; a monoclonal, N-terminus antibody, well characterized and specific for GluA2, and used previously for cochlea studies; Eybalin et al., 2004; Peppi et al., 2012; Martinez-Monedero, et al., 2012) labeling, a different labeling method was required because labeling was unsuccessful using the method mentioned above; tissue was fixed in 4% paraformaldehyde for 1 hr at 4°C, permeabilized with 0.5% Nonidet P-40 for 10 min at 4°C, and incubated in the primary antibody in PBS for 3 hr at room temperature (Martinez-Monedero, et al., 2012).

Triple labeling for GluK1, PSD-93 and Na^+/K^+-ATPase α3 was performed using tissues fixed in chilled, pure methanol for 30 min at -20°C (Meyer, et al., 2009), wherein secondary labeling for Na^+/K^+-ATPase α3 preceded primary labeling for GluK1 and PSD-93.

For mGluR7 (Imgenex, 1:500) labeling, cochlear tissue was fixed in 4% paraformaldehyde for 1 hr at 4°C, permeabilized wit h 0.5% Triton X-100 for 30 min and incubated in the primary antibody. We used an affinity-purified rabbit polyclonal antibody made from a synthetic peptide corresponding to the extracellular domain of human mGluR7 and shown to be reactive in rats; the general immunohistochemistry of this antibody in the cochlea has been described previously (Friedman et al., 2009).

3. Results

3.1. GluK5 is expressed in OHCs, cochlear ganglion cells and vestibular hair cells in adult

We performed X-gal staining on GluK5 KO mice to determine the cellular distribution of GluK5 in the cochlea and vestibule. GluK5 expression in cochlear hair cells in whole-mount cochleae showed developmental changes (Fig. 1A-C). Both IHCs (arrow) and OHCs (arrowhead) showed *lacZ* reactivity with equal intensity at P8 (Fig. 1A); but IHCs showed reduced reactivity at P14 (Fig. 1B) and reactivity was lost completely at 1.5 months old (Fig. 1C). On the other hand, OHCs maintained reactivity throughout maturation. Wild-type (WT) mouse cochleae showed no reactivity (Fig. 1D). We also performed X-gal staining on cochlear sections to show GluK5 expression distribution in the cochlear ganglion and vestibular organ in adult (1.5 months of age). Here we co-stained using DAB to visualize the immunoreactivity of anti-neurofilament kDa antibody (clone RT97) to discriminate type I/ type II cochlear ganglion cells or show the vestibular hair cell layer, because the cytoplasm of type II ganglion cells and calyces of type I vestibular hair cells labels intensely with RT97, whereas the cytoplasm of type I ganglion cells labels weakly (Dau and Wenthold, 1989; Romand, et al., 1988; Dechesne et al., 1994; Tonnaer et al. 2010). In the spiral ganglion, both type I (arrowheads) and type II (arrows) cells showed reactivity (Fig. 1E). In the utricle, the hair cell layer was identified by the intense staining, using RT97, of neurofilaments below the hair cells and within the Type I hair cell calyces (Fig. 1F,G), matching closely with previous descriptions of this staining pattern (Dechesne et al., 1994; Tonnaer et al. 2010). The blue X-gal staining included the entire hair cell area, although the individual hair cells were obscure in our preparations.

Hearing properties of GluK5 KO mice were examined, but we could not detect statistically significant difference in hearing threshold between KO and wild-type (WT) mice (supplementary Fig. S1). In addition, immunoreactivity for GluK5 was detected in cochleae from GluK5 KO mice (data not shown). We checked the specificity of the GluK5 antibody based on transfection of COS-7 cells with the GluK5 construct (supplementary Fig. S2) and BLAST sequence, which showed no other protein of rat origin has sequence homology with the immunogen of the antibody (data not shown). According to these data, we concluded that construction of the mutant construct, produced by the insertion of the *lacZ* gene, may have resulted in the synthesis and retention of part of the GluK5 molecule. The efficiency of the knockout of the GluK5 gene has not been tested sufficiently by the developers. In fact, a

recent study using GluK5 KO mice found no difference between KO and WT in electrophysiological findings and expression level of synaptic proteins (Yan et al., 2013).

Based on the X-gal staining pattern in cochleae from GluK5 KO mice as well as what is known from the literature (Peppi et al., 2012), we hypothesized that GluK5 and other KAR subunits (Lerma and Marques, 2013) are expressed in the postsynaptic membrane of afferent terminals in IHCs and also in both pre- and postsynaptic membranes of afferent terminals in OHCs.

3.2. AMPARs and KARs are expressed in IHC afferent synapses

To localize KARs in cochlear hair cells, we performed immunocytochemistry of GluA2 (for a control; previously described as GluR2) and all subunits of KARs using whole-mount adult rat cochleae. We used some synaptic markers for afferent terminals: ribeye/CtBP2 for presynaptic ribbons (Liberman et al., 2011; Huang et al., 2012) and PSD-93 for postsynaptic densities (Davies, et al., 2001). GluA2, a subunit of AMPARs, is well known to be expressed in the postsynaptic membrane of IHC afferent terminals using a polyclonal anti-GluA2/3 antibody (Matsubara, et al., 1996; Liberman, et al., 2011). Results from the present study using a monoclonal anti-GluA2 antibody were consistent with previous studies; GluA2 was juxtaposed to the synaptic ribbon (Fig. 2A) and mostly colocalized with the postsynaptic density (Fig. 2B). A higher labeling density of GluA2 was seen laterally than centrally in the synapses, so that it often formed a ring shape (Matsubara, et al., 1996; Meyer, et al., 2009).

GluK2 and GluK5 were the only KARs detected in IHC afferent synapses. Immunoreactivity for GluK2 formed a small punctate pattern, located in the center of afferent synaptic terminals, so that GluK2 was juxtaposed to synaptic ribbons (Fig. 2C) or the postsynaptic density (Fig. 2D). We confirmed the location of GluK2 in IHC afferent synapses using Na^+/K^+-ATPase α3. IHC afferent nerve membranes were labeled by Na^+/K^+-ATPase α3 (McLean, et al., 2009; Liberman, et al., 2011) and each punctum of GluK2 was located at the center of the afferent synaptic terminal (Fig. 2E). Some immunoreactivity for GluK2 was not juxtaposed to ribbon synapses in the IHC synaptic area (Fig. 2C, arrowhead). We tried double labeling for GluK2 and VAMP2 (Safieddine and Wenthold, 1999) to examine the possibility that GluK2 is also expressed in the IHC efferent terminals, but we could not obtain any result that would support the idea (data not shown). On the other hand, immunoreactivity for GluK5 showed a similar labeling pattern to that of GluA2. GluK5 was juxtaposed to the synaptic ribbon (Fig. 2F), mostly merged with the postsynaptic density (Fig. 2G) and distributed more laterally than centrally in the synapse.

High-power analysis of double-stained IHC afferent synapses revealed the detailed distribution of KARs in the synapses. We also used immunostaining of GluA2 for the purpose of comparison. GluA2, GluK2 and GluK5 were stained with synaptic markers (CtBP2/ribeye, PSD-93), and fluorescent signal intensity from side views and top views of the synapses were measured and visualized in Fig. 3. Averaged peak distance of various coupled signals measured in the side view is shown in Fig. 4. Each measured distance was compared with the distance between CtBP2 and PSD-93 (CtBP2-PSD93, a control distance) to show relative distances and similarities between the positions of the epitope sites for the

antibodies. The presynaptic synaptic ribbon and postsynaptic density were separated by a distance of nm (CtBP2-PSD93 in Fig. 4). From the top view, the ribbon synapse was located in the center of the synapse (Fig. 3). GluA2 labeling was close to labeling for PSD-93 and the distance (GluA2-PSD93, 50 nm) was significantly different from the control. This is consistent with the fact that AMPARs are expressed in the postsynaptic membrane. GluK5 labeling was juxtaposed to CtBP2, showing the same distance as the control, and colocalized with PSD-93 and GluA2. GluK5 and PSD-93 were colocalized in the synapse, indicating that GluK5 is also located in the postsynaptic membrane; this is consistent with the X-gal staining study showing that GluK5 is in the ganglion cells but not in the IHCs. Interestingly, GluA2 deviated slightly from GluK5 (GluA2-GluK5, 70 nm) and was closer to the synaptic ribbon (ribeye-GluA2, 200 nm; significantly shorter than the control), showing a different distribution of GluA2 and GluK5 inside the synapse. From the top view, GluK5 labeling distribution matched that of PSD-93 or GluA2, and a higher labeling density of GluK5 and GluA2 was seen more laterally than centrally in the synapse. Moreover, side views of GluK2 labeling sometimes showed double peaks in IHC afferent synapses. The first peak of GluK2 (P1 in Fig. 3) was far from postsynaptic GluA2 and PSD-93; the distance of GluK2 (P1)-GluA2 (220 nm) was almost the same as the control distance of CtBP2-PSD93, indicating that the first peak of GluK2 is in the presynaptic membrane or associated with synaptic ribbons. The second peak of GluK2 (P2 in Fig. 3) was close to postsynaptic GluA2 and PSD-93; the distance of GluK2(P2)-GluA2 and GluK2(P2)-PSD93 (50 nm) was almost the same as that of GluA2-PSD93, indicating that the second peak of GluK2 is in the postsynaptic membrane. The distance of CtBP2-GluK2 (150 nm) was an intermediate value between that of GluK2(P1)-GluA2 and GluK2(P2)-GluA2 (50 nm), probably because both GluK2 and CtBP2 labeled in small circular punctate patterns and, therefore, it was difficult to determine the exact side axis without a reference line. Both presynaptic GluK2 and postsynaptic GluK2 were located in the center of the synapse.

3.3. KARs are expressed in OHC afferent synapses and efferent synapses

We also examined expression of GluRs in OHCs using immunocytochemistry. Confocal z-stacks, followed by maximum intensity projections (Fig. 5A, B, C, E and H) or 3D reconstruction (Fig. 5D, F, G and I) were performed to visualize the entire synaptic region at the bottom of the OHCs. We used only the basal cochlear turn for imaging. First, we visualized terminals of OHC afferents and OHC efferents with PSD-93 and Na^+/K^+-ATPase α3 (McLean, et al., 2009), respectively. Small afferent terminals formed a C-shaped line at the base of OHCs on the strial face, and few of them were accompanied by a synaptic ribbon (Fig. 5A). OHC efferent terminals were larger boutons compared to afferent terminals, and 3 to 5 boutons were clumped at the base of OHCs and surrounded by afferent terminals (Fig. 5B). The anatomical relationship of afferent and efferent nerve terminals at the base of OHCs was confirmed by double staining of PSD-93 and synapsin (supplementary Fig. S3), and electron microscopy (supplementary Fig. S4).

Definitive immunoreactivity for GluA2 was not found in OHCs of adult rat cochlea (data not shown), although immunoreactivity for GluA2 was detected consistently in IHC afferent terminals. Among KAR subunits, immunoreactivity for GluK1, GluK2, and GluK5 was detected in OHC synaptic terminals. Small puncta of immunoreactivity for GluK2 were

colocalized with CtBP2 (Fig. 5C and D), indicating that these colocalized puncta were detected only in afferent terminals bearing synaptic ribbons (arrows in Fig. 5D). Distinctive immunoreactivity for GluK2 was also seen at the base of OHCs in a circular plaque pattern (Fig. 5D). Three to five plaques were clustered beneath OHCs, corresponding to the area where efferent terminals innervate (Fig. 5B). Immunoreactivity for GluK5 also was seen in the afferent terminal area of OHCs (Fig. 5E), but the expression pattern was slightly different from GluK2. GluK5 was detected in all afferent terminals, labeled by PSD-93 (Fig. 5E), and 1 or 2 larger and brighter puncta were included among them (arrows in Fig. 5F). This brighter immunoreactivity for GluK5 was associated with afferent terminals that also were immunoreactive for CtBP2, i.e., those bearing synaptic ribbons (arrows in Fig. 5G). In addition, immunoreactivity for GluK5 was clearly detected at the base of OHCs in the same pattern as that found for GluK2 (Fig. 5F and G), i.e., high immunoreactivity was associated with efferent terminals and at afferent terminals with synaptic ribbons. Unlike GluK2 and GluK5, immunoreactivity for GluK1 was found only in OHC efferent terminals, again in the same pattern as that found for GluK2 and GluK5. We successfully performed triple labeling for GluK1, PSD-93 for afferent terminals, and Na^+/K^+-ATPase $\alpha 3$ for membranes of efferent nerve boutons, using methanol fixation (Fig. 5H). GluK1 antibody did not label in afferent terminals, but labeled efferent nerve terminals in a circular pattern of plaques, similar to those seen in GluK2 and GluK5 immunoreactivity. Interestingly, several plaques were included in one terminal, indicating the position of individual active zones in the efferent terminal contact zone (Fig. 5I). Using paraformaldehyde fixation, we confirmed that immunoreactivity for GluK1 was not colocalized with afferent terminals and located only in the area where efferent nerves innervate (data not shown). We attempted double labeling with antibodies to GluK2 or GluK5, and the antibody to Na+/K+-ATPase a3, but were not successful because the labeling gave a high background.

3.4. KARs are expressed prominently in the early postnatal cochlea, but AMPARs show only minimal expression in OHC afferent terminals

Finally, we examined changes in the expression of GluA2 and KARs in OHC afferent terminals in P8 animals (Fig. 6). The basal cochlea precedes the apical cochlea in acquisition and maturation of mechanoelectric transduction (Waguespack, et al., 2007). We used whole turns of P8 rat cochleae and performed double immunolabeling for GluA2 or each subtype of KARs, with afferent synaptic markers (CtBP2/ribeye or PSD-93) to compare their expression between the apical turn (a) and the basal turn (b). We found a different expression pattern of OHC afferent terminals and the receptors between the apical turn and basal turns (Fig. 6A-N); quantification of the change in the ratio of ribeye/PSD-93, KAR/PSD-93, GluK2/CtBP2 and GluA2/ribeye is shown in Fig. 6O. In the apical turn (Fig. 6A), synaptic ribbons (ribeye) were mostly juxtaposed to the postsynaptic density (PSD-93) in the strial synaptic area of OHCs; about 80% of afferent synapses (n=21) were associated with synaptic ribbons (Fig. 6O). In the basal turn at P8 (Fig, 6B), however, the number of the afferent terminals accompanied by a synaptic ribbon was reduced to 50% (n=61), and only 30% of afferent terminals (n=45) were associated with ribbons in the adult (Fig. 5A; Fig. 6O), suggesting that the basal turn precedes the apical turn in the developmental process. In the apical turn, immunoreactivity for GluK1 (Fig. 6C), GluK2 (Fig. 6G and 6I), GluK3 (Fig. 6E) and GluK5 (Fig. 6K) was evident in OHC afferent terminals. However, in

the basal turn, GluK1 (Fig. 6D) and GluK3 (Fig. 6F) diminished to 5% and only GluK2 (Fig. 6H and 6J) and GluK5 (Fig. 6L) labeled (Fig. 6O), showing a pattern of expression close to that seen in the adult cochlea (Fig. 5). Immunoreactivity for GluK2 was colocalized with most afferent terminals (90%, *n*=24) in the apical turn (Fig. 6G), but only 40% of afferent terminals (*n*=38) were juxtaposed to GluK2 in the basal turn (Fig. 6H). On the other hand, immunoreactivity for GluK2 and CtBP2 was perfectly colocalized both in the apical turn (Fig. 6I) and basal turn (Fig. 6J), both at P8 and in the adult (Fig. 6O), showing that GluK2 is expressed in only those afferent synapses bearing synaptic ribbons as was demonstrated in the adult cochlea (Fig. 5D). Immunoreactivity for GluK5 was detected in all afferent terminals (as identified with PSD-93 labeling) both in the apical turn (Fig. 6K) and basal turn (Fig. 6L) at P8 (Fig. 6O); again, this is the same pattern that was demonstrated in the adult cochlea (Fig. 5F). We also tried immunolabeling for GluA2 with ribeye in P8 rat cochleae. Surprisingly, immunoreactivity for GluA2 was evident in afferent terminals and 90% of the synaptic ribbons (*n*=42; as identified with ribeye labeling) were juxtaposed to GluA2 labeling in the apical turn (Fig. 6M). In contrast, the number of synaptic ribbons with GluA2 decreased dramatically to 20% (*n*=42) in the basal turn (Fig. 6N), although we consistently detected immunoreactivity for GluA2 in IHC afferent terminals both in the apical and basal turn (data not shown). In adult, we could not obtain clear evidence of expression of GluA2 in OHC afferent synapses (0%, *n*=76; Fig. 6O).

4. Discussion

In this study (supplementary Fig. S5), we found that: 1) adult IHC afferent synapses have postsynaptic KARs containing GluK2 and GluK5 (in addition to AMPARs as described previously) and presynaptic KARs with GluK2. 2) The adult OHC afferent terminal GluRs are KARs containing GluK2 and GluK5. 3) At P8, OHC afferent terminals also have GluK1 and GluK3. 4) OHC efferent terminal synapses have KARs with GluK1, GluK2, and GluK5.

4.1. KARs in IHC afferents - pre and post

We found definitive evidence here for only two kinds of KAR subunits, GluK2 and GluK5, in close association with labeling for markers of the synaptic ribbon (CtBP2 or ribeye; Khimich et al., 2005; Huang et al., 2012) or PSD (PSD-93; Davies et al., 2001) at the IHC afferent synapses. In contrast, Peppi et al. (2012) showed that some puncta representing each of the 5 KAR subunits could colocalize with GluA2 puncta at the base of the IHCs of CBA/CaJ mice. We found that GluA2-immunoreactivity (using the same monoclonal antibody that was used in Peppi et al., 2012) produced some puncta that do not colocalize with the ribbon and PSD markers. This is expected since AMPAR labeling can include labeling in the cytoplasm of neurons and hair cells (Petralia and Wenthold, 1992; Petralia et al., 1997; Huang et al., 2012). At least some of the colocalization reported by Peppi et al. (2012) may not have been directly postsynaptic. This might explain why we found only two of the subunits specifically at the IHC afferent synapses. Our GluK4 antibody did not seem to work; therefore, we do not know if GluK4 is also at these synapses. Antibodies to the other two subunits, GluK1 and GluK3, labeled in specific locations in P8 animals (as did GluK1 in the adult), as discussed below. Thus, we believe that their absence here reflects a real absence from the adult IHCs. The lack of staining for GluK3 was expected because

Neidzielski and Wenthold (1995) found GluK3 to be completely absent from adult rat vestibulocochlear ganglion cells. It is not understood why Peppi et al. (2012) found GluK3 immunoreactivity at the adult mouse IHCs, but perhaps this may be due to species differences between rats and mice. We will consider this again below in relation to developmental changes. The postsynaptic labeling at IHC afferent synapses is well known for AMPARs (Matsubara et al., 1996). We show that GluK5 is postsynaptic in IHCs and forms a similar ring pattern of immunoreactivity (Matsubara et al., 1996; Meyer et al., 2009, 2012) although the pattern can vary (Liberman et al., 2011). Our X-gal staining that indicated GluK5 in adult Type I cochlear ganglion cells but not in IHCs supports the postsynaptic location of GluK5 in IHCs. In addition, while it is clear that GluA2 and GluK5 colocalize on the postsynaptic side of IHC afferent synapses, we noted that GluA2 localizes a little closer to the synaptic ribbon. Possibly this is due to different locations of the antibody epitopes, i.e., the epitope of the GluA2 antibody is in the extracellular N-terminus (Hollmann and Heinemann, 1994; Kew and Kemp, 2005), and thus in the synaptic cleft, while that of GluK5 is in the intracellular C-terminus. This postsynaptic colocalization of GluA2 and GluK5 suggests that GluK5-containing KARs could receive the same local concentration of glutamate as AMPARs in the IHC synapse. In contrast, GluK2 was found mainly centrally in the PSD, just adjacent to the ribbon. Responses to glutamate release will depend both on the local pattern of receptor distribution as well as on the binding affinity of different receptors (Hollmann and Heinemann, 1994; Kew and Kemp, 2005). In ribbon synapses of the retina, AMPARs and KARs show different patterns under the synapse in association with the multiple postsynaptic processes found there, so that one kind of AMPAR is directly central postsynaptic, adjacent to the ribbon, while another kind of AMPAR is found just peripheral to this where it colocalizes with KARs (Puller and Haverkamp, 2011). We also found direct colocalization of a second punctum of GluK2 with the ribbon, suggesting that GluK2 is both presynaptic and postsynaptic at the IHC afferent synapse. This is consistent with labeling of retinal ribbon synapses, where an antibody to GluK2/3 labels both postsynaptic and presynaptic (Harvey and Calkins, 2002). KARs of the brain are well known to localize on both presynaptic and postsynaptic membranes (Darstein et al., 2003; Contractor and Swanson, 2008). Presynaptic KARs can modulate the release of glutamate neurotransmitter (Contractor and Swanson, 2008; Andrade-Talavera et al., 2012; Lerma and Marques, 2013). GluK2 could be functional alone or form a heteromeric receptor complex with GluK4 if present in the IHC.

4.2. KARs are the main GluR in OHC afferents

As noted, our study is the first to identify the OHC afferent synapse GluR. OHCs in adult rats have several afferent terminals arranged in a C-pattern (shown here with an antibody to the PSD protein, PSD-93; Davies et al., 2001), with only one or two of them labeling with a synaptic ribbon antibody. Similarly, Huang et al. (2012) found only two or three puncta for CtBP2 at the base of the OHCs of C57/BL6 mice; and this was shown also in ultrastructural studies in the cat and guinea pig (Hashimoto and Kimura, 1988; Liberman et al., 1990). We found high levels of immunoreactivity for GluK2 and GluK5 in the one or two afferent terminals bearing synaptic ribbons, as well as lower levels of immunoreactivity for GluK5 in all the other afferent terminals that are not accompanied by synaptic ribbons. As noted above, this is consistent with a differential pattern of immunoreactivity for different KAR

subunits associated with synapses in the retina (Puller and Haverkamp, 2011). The pattern of immunoreactivity of GluK2 and GluK5 and their colocalization with CtBP2 and PSD-93 appeared to be similar to that seen for the IHCs. However, it was difficult to identify the exact position of the GluK2 and GluK5 from the side, as we did for the IHCs, due to the orientation of the OHCs and fewer number of synapses; so it is not clear if all of the immunoreactivity was postsynaptic or presynaptic or both. Our X-gal staining showed that GluK5 is present both in adult Type II cochlear ganglion cells (i.e., afferents postsynaptic to OHCs) and in OHCs, so it is possible that both sides of the synapse could contain GluK5 (i.e., to form heteromeric complexes of GluK2 and GluK5; Hollmann and Heinemann, 1994; Contractor and Swanson, 2008). In contrast to KARs, we did not see any clear evidence of GluA2 expression at adult OHC synapses. This is consistent with other studies that showed that AMPARs are absent from adult OHC synapses (Matsubara et al., 1996; Eybalin et al., 2004; Liberman et al., 2011). Huang et al. (2012) found uncommon immunoreactivity for GluR2/3 and rare for GluR4 in adult OHCs of C57/BL6 mice, but none of this colocalized with CtBP2. We will discuss this below.

4.3. Developmental change in KAR expression

In P8 rats, we found that synapses in OHC apical turns, which develop later than basal turns (Waguespack et al., 2007), labeled for all four KAR antibodies studied (GluK4 antibody did not label definitively, as noted), colocalizing with CTBP2 and PSD-93. Synaptic ribbons were more common in P8 rats compared to adults, so that most synapses contained both GluK2 and GluK5, as well as GluK1 and GluK3. Labeling for ribbon synapses in the P8 basal turn was similar to that seen in the adult (described above), with fewer synapses containing ribbons. A developmental decrease in synaptic ribbons labeled using CtBP2 has been described previously (C57/BL6 mice; Huang et al., 2012) for both IHCs (decrease by about half from P0-6 to P12-adult) and OHCs (have as many ribbons as IHCs by P6 and then decrease to 2-3 in P12-adult). The basal turn OHCs of rats show fewer puncta of GluK2 immunoreactivity, compared to the apical turn OHCs, corresponding to the lower CtBP2 immunoreactivity, and only rare labeling at synapses for GluK1 or GluK3 (none is found in the adults). More diverse KARs appear to be present at P8 than in the adult. Overall this suggests that KARs are a major GluR type of OHCs for both postnatal development and in adults.

We did find some immunoreactivity for the AMPAR subunit, GluA2 at OHC synapses in the P8 apical turn and less commonly, at those of the basal turn at P8, but none in the adult as noted. This corresponds to the findings of Huang et al. (2012) in which AMPARs are only associated with OHC synaptic ribbons in C57/BL6 mice from P0-6 but not in adults. Weisz et al. (2009, 2012) observed functional GluRs in OHC afferent dendrites in the apical turn of early postnatal rat cochleae (P5-P9). Evoked EPSCs recorded in OHC afferent nerves were much smaller in amplitude and slow in kinetics, compared to EPSCs recorded in IHC afferent nerves (Weisz et al., 2012), and were blocked by NBQX, which is an antagonist for AMPARs and KARs (Hollmann and Heinemann, 1994; Kew and Kemp, 2005; Contractor and Swanson, 2008). Thus we can speculate that the functional GluRs in type II afferents that Weisz et al. revealed represent a mixture of synaptic AMPARs and KARs; they could be distinguished using an AMPAR-specific antagonist such as GYKI53655 (Lerma, 2003).

Our data, in conjunction with published data on AMPARs, indicate that at least in the adult, KARs are found at OHC afferent synapses but AMPARs are not. The adult pattern of synaptic GluRs, with AMPARs and KARs at IHCs but only KARs at OHCs is consistent with the complex pattern of AMPARs and KARs found in different cell types of the retina (Puller et al., 2013).

4.4. KARs in OHC efferents

In addition to localization of GluK2 and GluK5 in adult OHC afferent synapses, we found immunoreactivity for GluK1, GluK2, and GluK5 associated with the active zones of efferent synapses. At least GluK1 appears to be found within the efferent terminal and thus is presynaptic at these synapses. There are two possible explanations for localization of KARs at the cholinergic efferent synapses. One is that the terminals co-release glutamate with acetylcholine. There are a number of cases of co-release of neurotransmitters in the retina and brain, including glutamate and acetylcholine (Ren et al., 2011; Hnasko and Edwards, 2012). The efferent terminals on OHCs are believed to release other neurotransmitter chemicals in addition to acetylcholine (Eybalin, 1993; Wersinger and Fuchs, 2011; Elgoyhen and Katz, 2012). However, there is no evidence that glutamate is released from the OHC efferent terminals (Eybalin, 1993; Wersinger and Fuchs, 2011; Elgoyhen and Katz, 2012). It is most likely that these KARs respond to glutamate released from the OHC to help modulate release of the neurotransmitter acetylcholine from the efferent terminals. We already have discussed presynaptic KARs at afferent terminals, and their role in modulation of glutamate release has been studied in the CNS (Contractor and Swanson, 2008; Andrade-Talavera et al., 2012). KARs tend to be widespread outside of the postsynaptic membrane of glutamatergic synapses, including presynaptic, perisynaptic and extrasynaptic membranes (Darstein et al, 2003; Contractor and Swanson, 2008; Puller and Haverkamp, 2011). In the retina, KARs are found in desmosome-like junctions at a substantial distance from the ribbon synapse active zone (Puller and Haverkamp, 2011). There are wide spaces between cell processes at the base of the OHCs, and the glutamate/aspartate transporter GLAST is found on the surface of the surrounding Deiters' cell processes that extend well beyond the afferent and efferent terminals (Furness et al., 2002). This suggests that there is substantial spillover of glutamate into the surrounding area that could reach the efferent synapses that are adjacent to the afferent synapses. Glutamate spillover and spread is an important mechanism for synaptic modulation in many parts of the CNS (Nishiyama and Linden, 2007; Hires et al., 2008; Szapiro and Barbour, 2009; Petralia et al., 2010; Petralia, 2012. Szmajda and DeVries, 2011). Typically in the CNS, cholinergic terminals form complexes with glutamatergic terminals, as is found here with hair cells. Often these arrangements include presynaptic acetylcholine receptors on the glutamatergic terminals, so that acetylcholine modulates glutamate release (e.g., Garduño et al., 2012; Wang et al., 2012). But it is not clear if the opposite happens, i.e., glutamate modulating release of acetylcholine. This may occur in the frog cholinergic neuromuscular junction where metabotropic GluRs may be presynaptic (Pinard et al., 2003). A metabotropic GluR, mGluR7, has been associated with human hearing loss (Friedman, et al., 2009; Newman, et al., 2012). Interestingly, our preliminary study revealed OHC efferent nerve boutons stained with mGluR7 (Supplementary figure S6); these might be presynaptic mGluRs of the efferent terminals, as mGluR7 is predominantly presynaptic in the CNS (Shigemoto et al., 1997).

4.5. Functional Implications

KARs probably have modulatory roles at IHC afferent synapses, affecting both release of glutamate from the IHC and the postsynaptic response. The present study shows that presynaptic KARs (GluK2) and postsynaptic KARs (GluK2/GluK5) are present in IHC afferent synapses. It is known that presynaptic KARs modulate neurotransmitter release in a bidirectional manner in the brain (Lerma, 2003). Delaney and Jahr (2002) reported that at parallel fiber synapses in the cerebellum, synaptically released glutamate activates presynaptic KARs at the fibers and facilitates glutamate release with low-frequency stimulation. By contrast, the synapses onto the interneurons are depressed with high-637 frequency stimulation. Postsynaptic KARs also are thought to regulate neuronal excitability, probably providing integrative capacities for information transfer unfilled by other GluRs (Lerma and Marques, 2013). Thus, presynaptic and postsynaptic KARs in IHC/type I afferent synapses may have a role in regulation of transmission of acoustic stimulation or prevention of acoustic injury when there is excessive acoustic input.

More importantly, in OHC afferent synapses, KARs appear to be the major glutamate receptor type, and may be the only type. The present study showed that heteromeric KARs (GluK2/GluK5) are expressed in functional OHC afferent synapses associated with synaptic ribbons. Although we could not distinguish the side of the synapse where KARs are expressed in OHC afferent synapses, KARs exist at least in the postsynaptic side, because glutamatergic EPSCs are recorded in type II afferent dendrites (Weisz et al., 2009; 2012). It is known that maximal stimulation of OHCs is necessary for excitation of type II afferents (Weisz et al., 2012), and type II afferents respond only to the loudest, potentially traumatic sounds (Robertson, 1984; Brown, 1994; Robertson et al., 1999). Our morphological findings are consistent with these physiological suggestions because KAR-mediated small EPSCs (Lerma and Marques, 2013) should require repetitive synaptic activation and summated membrane potentials to trigger an action potential in type II afferent fibers. Moreover, we found evidence that ionotropic and/or metabotropic KARs are expressed in the OHC efferent synaptic cleft or on the bouton membrane. Glutamate spillover, which will depend on the magnitude of acoustic stimulation and uptake capacity of Deiter's cells, may act on KARs expressed in the OHC synaptic area and modulate normal OHC function or suppress excessive cochlear amplification. Further physiological examination using a specific antagonist for AMPARs would elucidate the existence and function of KARs in OHC synapses.

Materials & Methods

Auditory testing

Auditory testing was performed at 1.5, 3 and 5 months of age. At the start of a test session, the mouse was anesthetized via an intra-peritoneal (IP) injection of ketamine (100 mg/ml) and dexdomitor (0.5 mg/ml). The mouse was placed in a sound-treated booth on a heating plate connected to a temperature controller and rectal probe in order to maintain the mouse's temperature near 37°C. Distortion-product otoacoustic emissions (DPOAEs) and auditory brainstem responses (ABRs) were measured using hardware (RZ6 Multi I/O processor) and software (BioSigRz, v. 5.1) from Tucker-Davis Technologies (TDT; Alachua, FL, USA).

DPOAEs were measured first in both ears. The DPOAE measurement probe system consisted of two TDT MF-1 speakers coupled to an ER-10B+ microphone (Etymotic, Elk Grove Village, IL). The microphone was coupled to the mouse's ear using a modified pipette tip. The intensity of the two primary tones was held constant at f_1 = 65 dBpeSPL and f_2 = 55 dBpeSPL, while the frequencies of the tones were varied such that f_2 = 4 to 44.8 kHz (5 pts/octave) and f2/f1 = 1.25. The resulting $2f_1$-f_2 DPOAE amplitudes were examined as a function of f_2 (DPgram) with mean noise floor calculated from three points sampled above and three points sampled below the $2f_1$-f_2 frequency. The TDT system provides the output in dBV; therefore, data were converted to dBpeSPL offline.

Following DPOAE testing, ABR thresholds were determined for the right ear only at 8, 16, 22.4, 32, and 40 kHz. Subdermal needle electrodes were placed at the vertex of the head and beneath each pinna, with the non-test (left) ear serving as the ground. Blackman-gated tone-burst stimuli (3 msec duration, 29.9/sec, alternating polarity) were delivered to the right ear via PVC tubing terminating in a modified pipette tip attached to a TDT MF-1 speaker. Responses were amplified (20×) and filtered (0.3 - 3k Hz) and 512-1024 artifact-free responses were averaged for each waveform. Thresholds were determined by visual inspection of stacked waveforms for the lowest level at which any repeatable wave could be obtained. Stimulus intensities were decreased in 10-dB steps until no response was noted and then increased in 5-dB steps to determine the threshold. At least two waveforms (1024 sweeps each) were obtained for stimulus levels at and near threshold to ensure repeatability of the response. When no response was detectable at the highest stimulus level tested (90 dBpeSPL), the threshold was designated as 100 dBpeSPL for subsequent analyses.

Supplementary Material

Refer to Web version on PubMed Central for supplementary material.

Acknowledgments

This work was supported by the Intramural Research Program of the NIDCD at NIH. We also thank Dr. Stephan Brenowitz for reviewing the manuscript, and Dr. Kai Chang for advice related to the GluK5 mutant mouse.

References

Andrade-Talavera Y, Duque-Feria P, Negrete-Díaz JV, Sihra TS, Flores G, Rodríguez-Moreno A. Presynaptic kainate receptor-mediated facilitation of glutamate release involves Ca2+ -calmodulin at mossy fiber-CA3 synapses. J Neurochem. 2012; 122:891–899. [PubMed: 22731109]

Bianchi LM, Dinsio K, Davoli K, Gale NW. Lac z Histochemistry and immunohistochemistry reveal ephrin-B ligand expression in the inner ear. J Histochem Cytochem. 2002; 50:1641–1645. [PubMed: 12486086]

Brown MC. Antidromic responses of single units from the spiral ganglion. J Neurophysiol. 1994; 71:1835–1847. [PubMed: 8064351]

Contractor, A.; Swanson, GT. Kainate receptors. In: Gereau, RW.; Swanson, GT., editors. The Glutamate Receptors. Humana Press; 2008. p. 99-158.

Copits BA, Swanson GT. Dancing partners at the synapse: auxiliary subunits that shape kainate receptor function. Nat Rev Neurosci. 2012; 13:675–686. [PubMed: 22948074]

Corradi A, Croci L, Broccoli V, Zecchini S, Previtali S, Wurst W, Amadio S, Maggi R, Quattrini A, Consalez GG. Hypogonadotropic hypogonadism and peripheral neuropathy in Ebf2-null mice. Development. 2003; 130:401–410. [PubMed: 12466206]

Darstein M, Petralia RS, Swanson GT, Wenthold RJ, Heinemann SF. Distribution of kainate receptor subunits at hippocampal mossy fiber synapses. J Neurosci. 2003; 23:8013–8019. [PubMed: 12954862]

Dau J, Wenthold RJ. Immunocytochemical localization of neurofilament subunits in the spiral ganglion of normal and neomycin-treated guinea pigs. Hear Res. 1989; 42:253–263. [PubMed: 2606806]

Davies C, Tingley D, Kachar B, Wenthold RJ, Petralia RS. Distribution of members of the PSD-95 family of MAGUK proteins at the synaptic region of inner and outer hair cells of the guinea pig cochlea. Synapse. 2001; 40:258–268. [PubMed: 11309841]

Dechesne CJ, Scarfone E, Atger P, Desmadryl G. Neurofilament proteins form an annular superstructure in guinea-pig type I vestibular hair cells. J Neurocytol. 1994; 23:631–640. [PubMed: 7836957]

Delaney AJ, Jahr CE. Kainate receptors differentially regulate release at two parallel fiber synapses. Neuron. 2002; 36:475–482. [PubMed: 12408849]

Eybalin M. Neurotransmitters and neuromodulators of the mammalian cochlea. Physiol Rev. 1993; 73:309–373. [PubMed: 8097330]

Eybalin M, Caicedo A, Renard N, Ruel J, Puel JL. Transient Ca2+- permeable AMPA receptors in postnatal rat primary auditory neurons. Eur J Neurosci. 2004; 20:2981–2989. [PubMed: 15579152]

Frerking M, Ohliger-Frerking P. AMPA receptors and kainate receptors encode different features of afferent activity. J Neurosci. 2002; 22:7434–7443. [PubMed: 12196565]

Friedman RA, Van Laer L, Huentelman MJ, Sheth SS, Van Eyken E, Corneveaux JJ, Tembe WD, Halperin RF, Thorburn AQ, Thys S, Bonneux S, Fransen E, Huyghe J, Pyykkö I, Cremers CW, Kremer H, Dhooge I, Stephens D, Orzan E, Pfister M, Bille M, Parving A, Sorri M, Van de Heyning PH, Makmura L, Ohmen JD, Linthicum FH Jr, Fayad JN, Pearson JV, Craig DW, Stephan DA, Van Camp G. GRM7 variants confer susceptibility to age-related hearing impairment. Hum Mol Genet. 2009; 18:785–796. [PubMed: 19047183]

Furness DN, Hulme JA, Lawton DM, Hackney CM. Distribution of the glutamate/aspartate transporter GLAST in relation to the afferent synapses of outer hair cells in the guinea pig cochlea. J Assoc Res Otolaryngol. 2002; 3:234–247. [PubMed: 12382100]

Garduño J, Galindo-Charles L, Jiménez-Rodríguez J, Galarraga E, Tapia D, Mihailescu S, Hernandez-Lopez S. Presynaptic α4β2 nicotinic acetylcholine receptors increase glutamate release and serotonin neuron excitability in the dorsal raphe nucleus. J Neurosci. 2012; 32:15148–15157. [PubMed: 23100436]

Glowatzki E, Fuchs PA. Transmitter release at the hair cell ribbon synapse. Nat Neurosci. 2002; 5:147–154. [PubMed: 11802170]

Grati M, Shin JB, Weston MD, Green J, Bhat MA, Gillespie PG, Kachar B. Localization of PDZD7 to the stereocilia ankle-link associates this scaffolding protein with the Usher syndrome protein network. J Neurosci. 2012; 32:14288–14293. [PubMed: 23055499]

Harvey DM, Calkins DJ. Localization of kainate receptors to the presynaptic active zone of the rod photoreceptor in primate retina. Vis Neurosci. 2002; 19:681–692. [PubMed: 12507334]

Hashimoto S, Kimura RS. Computer-aided three-dimensional reconstruction and morphometry of the outer hair cells of the guinea pig cochlea. Acta Otolaryngol. 1988; 105:64–74. [PubMed: 3341163]

Hires SA, Zhu Y, Tsien RY. Optical measurement of synaptic glutamate spillover and reuptake by linker optimized glutamate-sensitive fluorescent reporters. Proc Natl Acad Sci U S A. 2008; 105:4411–4416. [PubMed: 18332427]

Hnasko TS, Edwards RH. Neurotransmitter corelease: mechanism and physiological role. Annu Rev Physiol. 2012; 74:225–243. [PubMed: 22054239]

Hollmann M, Heinemann S. Cloned glutamate receptors. Annu Rev Neurosci. 1994; 17:31–108. [PubMed: 8210177]

Huang LC, Barclay M, Lee K, Peter S, Housley GD, Thorne PR, Montgomery JM. Synaptic profiles during neurite extension, refinement and retraction in the developing cochlea. Neural Dev. 2012; 7:38. [PubMed: 23217150]

Kew JN, Kemp JA. Ionotropic and metabotropic glutamate receptor structure and pharmacology. Psychopharmacology (Berl). 2005; 179:4–29. [PubMed: 15731895]

Khimich D, Nouvian R, Pujol R, Tom Dieck S, Egner A, Gundelfinger ED, Moser T. Hair cell synaptic ribbons are essential for synchronous auditory signalling. Nature. 2005; 434:889–894. [PubMed: 15829963]

LePage EL. Functional role of the olivo-cochlear bundle: a motor unit control system in the mammalian cochlea. Hear Res. 1989; 38:177–198. [PubMed: 2708162]

Lerma J. Roles and rules of kainate receptors in synaptic transmission. Nat Rev Neurosci. 2003; 4:481–495. [PubMed: 12778120]

Lerma J, Marques JM. Kainate receptors in health and disease. Neuron. 2013; 80:292–311. [PubMed: 24139035]

Liberman LD, Wang H, Liberman MC. Opposing gradients of ribbon size and AMPA receptor expression underlie sensitivity differences among cochlear-nerve/hair-cell synapses. J Neurosci. 2011; 31:801–808. [PubMed: 21248103]

Liberman MC. Morphological differences among radial afferent fibers in the cat cochlea: an electron-microscopic study of serial sections. Hear Res. 1980; 3:45–63. [PubMed: 7400048]

Liberman MC. Single-neuron labeling in the cat auditory nerve. Science. 1982; 216:1239–1241. [PubMed: 7079757]

Liberman MC, Brown MC. Physiology and anatomy of single olivocochlear neurons in the cat. Hear Res. 1986; 24:17–36. [PubMed: 3759672]

Liberman MC, Dodds LW, Pierce S. Afferent and efferent innervation of the cat cochlea: quantitative analysis with light and electron microscopy. J Comp Neurol. 1990; 301:443–460. [PubMed: 2262601]

Maison SF, Rosahl TW, Homanics GE, Liberman MC. Functional role of GABAergic innervation of the cochlea: phenotypic analysis of mice lacking GABA(A) receptor subunits alpha 1, alpha 2, alpha 5, alpha 6, beta 2, beta 3, or delta. J Neurosci. 2006; 26:10315–10326. [PubMed: 17021187]

Maison SF, Casanova E, Holstein GR, Bettler B, Liberman MC. Loss of GABAB receptors in cochlear neurons: threshold elevation suggests modulation of outer hair cell function by type II afferent fibers. J Assoc Res Otolaryngol. 2009; 10:50–63. [PubMed: 18925381]

Marrocco J, Mairesse J, Ngomba RT, Silletti V, Van Camp G, Bouwalerh H, Summa M, Pittaluga A, Nicoletti F, Maccari S, Morley-Fletcher S. Anxiety-815 like behavior of prenatally stressed rats is associated with a selective reduction of glutamate release in the ventral hippocampus. J Neurosci. 2012; 32:17143–17154. [PubMed: 23197707]

Martinez-Monedero R, Weisz C, Chatlani S, Fuchs P, Glowatzki E. GluR2 receptors at the IHC and OHC afferent synapse in the rat cochlea. ARO Annual MidWinter Meeting. 2012; 35:135. abstract.

Matsubara A, Laake JH, Davanger S, Usami S, Ottersen OP. Organization of AMPA receptor subunits at a glutamate synapse: a quantitative immunogold analysis of hair cell synapses in the rat organ of Corti. J Neurosci. 1996; 16:4457–4467. [PubMed: 8699256]

McLean WJ, Smith KA, Glowatzki E, Pyott SJ. Distribution of the Na,K-827 ATPase alpha subunit in the rat spiral ganglion and organ of corti. J Assoc Res Otolaryngol. 2009; 10:37–49. [PubMed: 19082858]

Meyer AC, Frank T, Khimich D, Hoch G, Riedel D, Chapochnikov NM, Yarin YM, Harke B, Hell SW, Egner A, Moser T. Tuning of synapse number, structure and function in the cochlea. Nat Neurosci. 2009; 12:444–453. [PubMed: 19270686]

Moser T, Brandt A, Lysakowski A. Hair cell ribbon synapses. Cell Tis Res. 2006; 326:347–359.

Nasu-Nishimura Y, Hurtado D, Braud S, Tang TT, Isaac JTR, Roche KW. Identification of an endoplasmic reticulum-retention motif in an intracellular loop of the kainate receptor subunit KA2. J Neurosci. 2006; 26:7014–7021. [PubMed: 16807331]

Newman DL, Fisher LM, Ohmen J, Parody R, Fong CT, Frisina ST, Mapes F, Eddins DA, Robert Frisina D, Frisina RD, Friedman RA. GRM7 variants associated with age-related hearing loss based on auditory perception. Hear Res. 2012; 294:125–132. [PubMed: 23102807]

Niedzielski AS, Wenthold RJ. Expression of AMPA, kainate, and NMDA receptor subunits in cochlear and vestibular ganglia. J Neurosci. 1995; 15:2338–2353. [PubMed: 7891171]

Nishiyama H, Linden DJ. Pure spillover transmission between neurons. Nat Neurosci. 2007; 10:675–677. [PubMed: 17525760]

Peppi M, Landa M, Sewell WF. Cochlear kainate receptors. J Assoc Res Otolaryngol. 2012; 13:199–208. [PubMed: 22231646]

Petralia RS. Distribution of extrasynaptic NMDA receptors on neurons. Scientific World Journal. 2012; 2012:267120. [PubMed: 22654580]

Petralia RS, Wang YX, Hua F, Yi Z, Zhou A, Ge L, Stephenson FA, Wenthold RJ. Organization of NMDA receptors at extrasynaptic locations. Neuroscience. 2010; 167:68–87. [PubMed: 20096331]

Petralia RS, Wang YX, Mayat E, Wenthold RJ. Glutamate receptor subunit 2-selective antibody shows a differential distribution of calcium-impermeable AMPA receptors among populations of neurons. J Comp Neurol. 1997; 385:456–476. [PubMed: 9300771]

Petralia RS, Wenthold RJ. Light and electron immunocytochemical localization of AMPA-selective glutamate receptors in the rat brain. J Comp Neurol. 1992; 318:329–354. [PubMed: 1374769]

Petralia RS, Wenthold RJ. Immunocytochemistry of NMDA receptors. Methods Mol Biol. 1999; 128:73–92. [PubMed: 10320974]

Pinard A, Lévesque S, Vallée J, Robitaille R. Glutamatergic modulation of synaptic plasticity at a PNS vertebrate cholinergic synapse. Eur J Neurosci. 2003; 18:3241–3250. [PubMed: 14686898]

Puller C, Haverkamp S. Cell-type-specific localization of protocadherin β16 at AMPA and AMPA/Kainate receptor-containing synapses in the primate retina. J Comp Neurol. 2011; 519:467–479. [PubMed: 21192079]

Puller C, Ivanova E, Euler T, Haverkamp S, Schubert T. Off bipolar cells express distinct types of dendritic glutamate receptors in the mouse retina. Neuroscience. 2013; 243:136–148. [PubMed: 23567811]

Ren J, Qin C, Hu F, Tan J, Qiu L, Zhao S, Feng G, Luo M. Habenula “cholinergic” neurons co-release glutamate and acetylcholine and activate postsynaptic neurons via distinct transmission modes. Neuron. 2011; 69:445–452. [PubMed: 21315256]

Robertson D. Horseradish peroxidase injection of physiologically characterized afferent and efferent neurones in the guinea pig spiral ganglion. Hear Res. 1984; 15:113–121. [PubMed: 6490538]

Robertson D, Sellick PM, Patuzzi R. The continuing search for outer hair cell afferents in the guinea pig spiral ganglion. Hear Res. 1999; 136:151–158. [PubMed: 10511634]

Romand R, Hafidi A, Despres G. Immunocytochemical localization of neurofilament protein subunits in the spiral ganglion of the adult rat. Brain Res. 1988; 462:167–173. [PubMed: 3141005]

Ruel J, Chen C, Pujol R, Bobbin RP, Puel JL. AMPA-preferring glutamate receptors in cochlear physiology of adult guinea-pig. J Physiol. 1999; 518:667–680. [PubMed: 10420005]

Safieddine S, El-Amraoui A, Petit C. The auditory hair cell ribbon synapse: From assembly to function. Annu Rev Neurosci. 2012; 35:509–528. [PubMed: 22715884]

Safieddine S, Wenthold RJ. SNARE complex at the ribbon synapses of cochlear hair cells: analysis of synaptic vesicle- and synaptic membrane-associated proteins. Eur J Neurosci. 1999; 11:803–812. [PubMed: 10103074]

Shigemoto R, Kinoshita A, Wada E, Nomura S, Ohishi H, Takada M, Flor PJ, Neki A, Abe T, Nakanishi S, Mizuno N. Differential presynaptic localization of metabotropic glutamate receptor subtypes in the rat hippocampus. J Neurosci. 1997; 17:7503–7522. [PubMed: 9295396]

Spoendlin H. Innervation patterns in the organ of corti of the cat. Acta Otolaryngol. 1969; 67:239–254. [PubMed: 5374642]

Szapiro G, Barbour B. Parasynaptic signalling by fast neurotransmitters: the cerebellar cortex. Neuroscience. 2009; 162:644–655. [PubMed: 19358875]

Szmajda BA, Devries SH. Glutamate spillover between mammalian cone photoreceptors. J Neurosci. 2011; 31:13431–13441. [PubMed: 21940436]

Tonnaer EL, Peters TA, Curfs JH. Neurofilament localization and phosphorylation in the developing inner ear of the rat. Hear Res. 2010; 267:27–35. [PubMed: 20430081]

Waguespack J, Salles FT, Kachar B, Ricci AJ. Stepwise morphological and functional maturation of mechanotransduction in rat outer hair cells. J Neurosci. 2007; 27:13890–13902. [PubMed: 18077701]

Wedemeyer C, Zorrilla de San Martín J, Ballestero J, Gómez-Casati ME, Torbidoni AV, Fuchs PA, Bettler B, Elgoyhen AB, Katz E. Activation of presynaptic GABA(B(1a,2)) receptors inhibits synaptic transmission at mammalian inhibitory cholinergic olivocochlear-hair cell synapses. J Neurosci. 2013; 33:15477–15487. [PubMed: 24068816]

Weisz C, Glowatzki E, Fuchs P. The postsynaptic function of type II cochlear afferents. Nature. 2009; 461:1126–1129. [PubMed: 19847265]

Weisz CJ, Lehar M, Hiel H, Glowatzki E, Fuchs PA. Synaptic transfer from outer hair cells to type II afferent fibers in the rat cochlea. J Neurosci. 2012; 32:9528–9536. [PubMed: 22787038]

Wersinger E, McLean WJ, Fuchs PA, Pyott SJ. BK channels mediate cholinergic inhibition of high frequency cochlear hair cells. PLoS One. 2010; 5:e13836. [PubMed: 21079807]

Wersinger E, Fuchs PA. Modulation of hair cell efferents. Hear Res. 2011; 279:1–12. [PubMed: 21187136]

Yan D, Yamasaki M, Straub C, Watanabe M, Tomita S. Homeostatic control of synaptic transmission by distinct glutamate receptors. Neuron. 2013; 78:687–699. [PubMed: 23719165]

Abbreviations

ACh	acetylcholine
GABA	Gamma amino butyric acid
AMPAR	AMPA-type glutamate receptor
GluR	glutamate receptor
KAR	kainate-type glutamate receptor
IHC	inner hair cell
MOC	medial olivocochlear
OHC	outer hair cell

Highlights

- Adult IHC afferent synapses have postsynaptic KARs with GluK2&5 + presynaptic GluK2.
- Adult OHC afferent terminal GluRs are KARs containing GluK2 and GluK5.
- At P8, OHC afferent terminals also have GluK1 and GluK3.
- Adult OHC efferent terminal synapses have KARs with GluK1, GluK2, and GluK5.

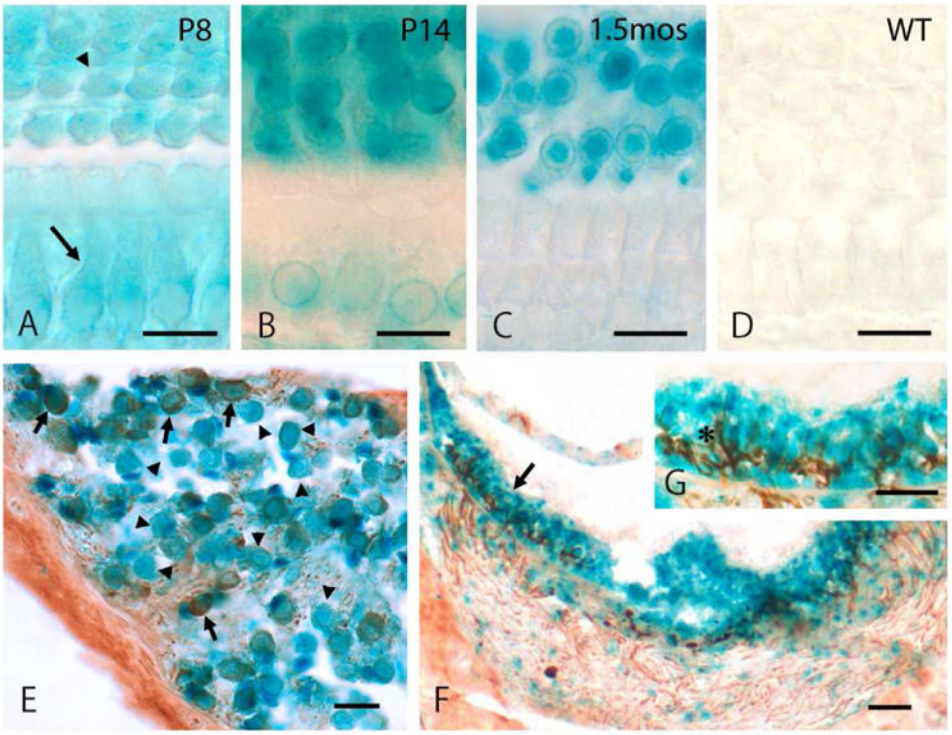

Fig. 1.

GluK5 expression in OHCs, cochlear ganglion cells and vestibular hair cells. (A, B, C, D) X-gal staining was performed on whole-mount cochleae from GluK5 knockout (KO) mice at postnatal day (P) 8 (A), P14 (B) and 1.5 months of age (C, D). OHCs (arrowhead) maintain reactivity throughout development but IHCs (arrow) lose reactivity in the adult. No reactivity is detected in cochleae from wild-type (WT) mice (D). (E, F, G) X-gal staining, plus DAB staining for a neurofilament protein (antibody clone RT97), was performed using inner ear sections at 1.5 months of age. In cochlea, both type I and type II ganglion cells show *lacZ* reactivity. Type II cells (arrows) are stained intensely in the cytoplasm with RT97, compared to type I cells (arrowheads) (E). In the utricle (F,G), reactivity is seen throughout the hair cell layer, identified by intense staining in nerve fibers and type I hair cell calyces with RT97 (asterisk in G, which is a 2× magnification of the area in F indicated by an arrow). Scale bar is 20 μm.

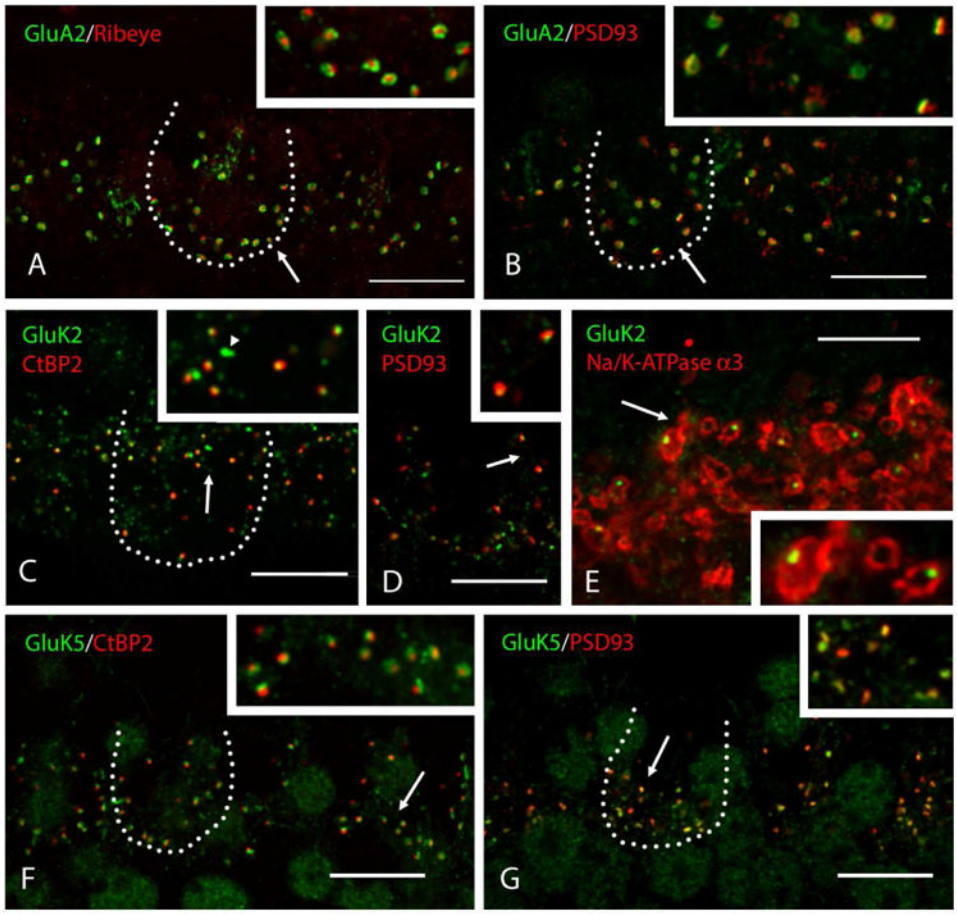

Fig. 2.

AMPAR and KAR expression in IHC afferent synapses. The basal turn of whole-966 mount adult rat cochleae was used for imaging. Representative IHC bodies are outlined with a dotted line. Inset in each panel shows a higher magnification (2×) of synapses in the area indicated by the arrow. (A, B) GluA2 is detected in IHC afferent synapses, coupled with the presynaptic ribbon marker, ribeye (A) or postsynaptic marker, PSD-93 (B). Distribution of GluA2 is colocalized with PSD-93 and a higher labeling density is seen laterally than centrally in the synapse, so that it often forms a ring shape. (C, D, E) GluK2 is detected in IHC afferent synapses. The small puncta of GluK2 are located in the center of synaptic terminals and are coupled with CtBP2 (C) or PSD-93 (D). Some signals of GluK2 are not associated with a synaptic marker (arrowhead in C). Localization of GluK2 in the center of synaptic terminals is confirmed by double staining with Na^+/K^+-ATPase α3, indicating the IHC afferent nerve membranes (E). (F, G) GluK5 is detected in IHC afferent synapses, coupled with CtBP2 (F) or PSD-93 (G). Puncta of GluK5 are generally larger, compared to those for GluK2, and colocalize more completely with PSD-93 (G). Scale bar is 10 μm (A-D, F-G) and 5 μm (E).

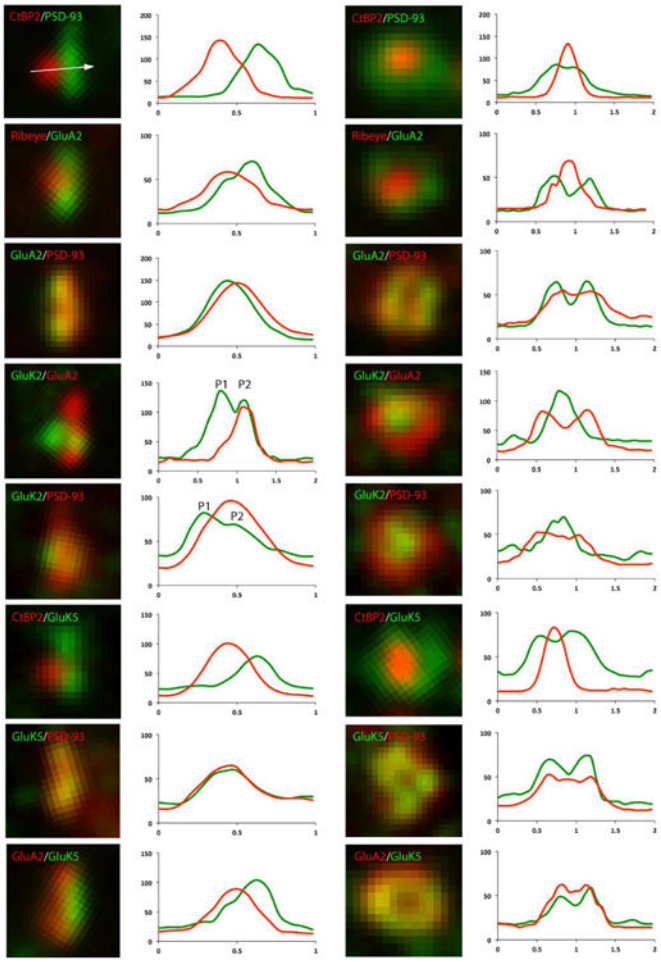

Fig. 3.

High power analysis of GluRs in IHC afferent synapses. Afferent synapses labeled with GluRs (GluA2, GluK2, GluK5) and synaptic markers (CtBP2/ribeye, PSD-93) are seen from the side (left column) and the top (right column). Signal intensity in relation to distance (μm) in X-axis is traced on the right of each example. The white arrow in the micrograph on the top of the left column (CtBP2/PSD-93) illustrates the position and direction of the sampling line used to measure the intensity trace. All samples were prepared and stained using the same experimental conditions and data were obtained only from the basal cochlear turn. Note that immunoreactivity for GluK2 sometimes shows double peaks in the side view (P1, presynaptic side; P2, postsynaptic side). Top view shows that GluA2 and GluK5 distribute more laterally (overlapped with PSD-93), and GluK2 locates more centrally in the synapse.

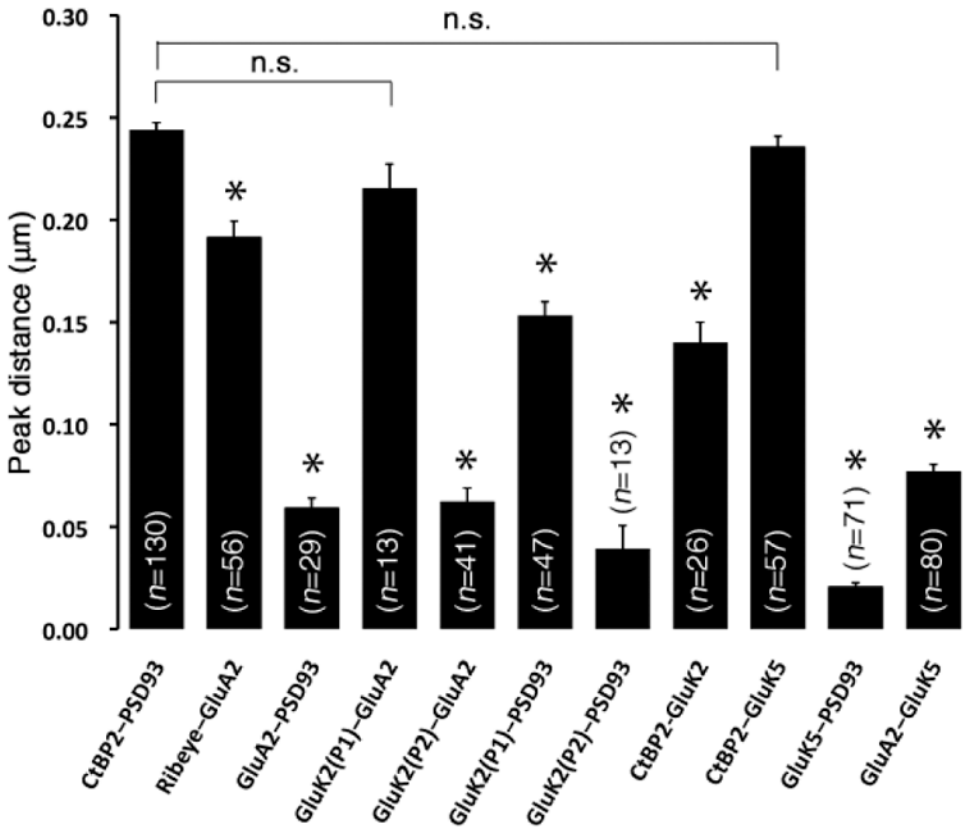

Fig. 4.

Localization of GluRs in IHC afferent synapses. Distance between fluorescent peaks was measured for each pattern of the staining in Fig. 3. Each bar represents the mean distance ± the standard error of the mean (SEM) for the indicated number of synapses measured (n). Each distance was compared with a control distance between CtBP2 and PSD-93 (CtBP2-PSD93, nm); asterisk indicates a statistically significant difference by *t*-test ($p<0.001$) and n.s. indicates statistically not significant. GluA2 and GluK5 are close to PSD-93 (see GluA2-PSD93, GluK5-PSD93). Note that GluA2 and GluK5 show different distributions in the postsynaptic area (see GluA2-GluK5) and GluK5 is closer to PSD-93. The first peak of GluK2 (P1) is far from GluA2 or PSD-93 (see GluK2(P1)-GluA2, GluK2(P1)-PSD93) and the peak distance (220nm, 160nm, respectively) is close to the control distance. The second peak of GluK2 (P2) is close to GluA2 or PSD-93 (see GluK2(P2)-GluA2, GluK2(P2)-PSD93), showing a similar distance to that of GluA2-PSD93 (60 nm, 40 nm, 60 nm, respectively).

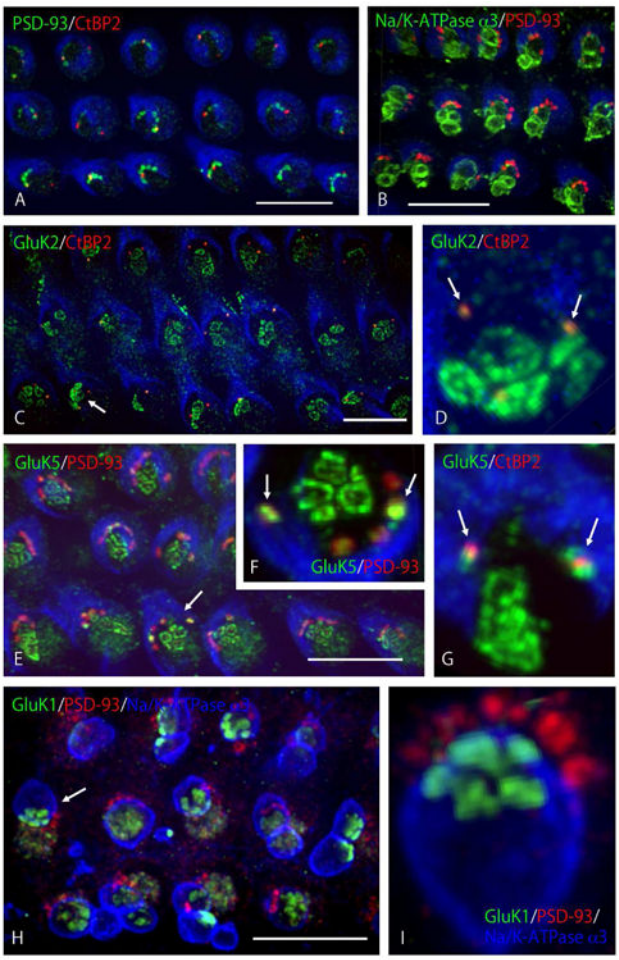

Fig. 5.

KAR expression in OHC synapses. The basal turn of whole-mount adult rat cochleae was used for imaging. Z-stack imaging was processed further by maximum intensity projection (A, B, C, E, H) or 3D reconstruction (D, F, G, I) to represent the entire synaptic area at the bottom of OHCs. Three rows of OHCs are shown with strial side facing up (A, B, C, E, H). (A, B) Afferent and efferent synapses are found at the bottom of OHCs. 3-7 afferent terminals (PSD-93) innervate OHCs from the strial side, arranged in a C-shape, and only 1 or 2 terminals bear synaptic ribbons (A). 1–4 efferent terminals (Na^+/K^+-ATPase α3) contact the bottom of OHCs, surrounded by afferent terminals (B). (C, D) GluK2 is detected in OHC afferent and efferent synaptic regions. GluK2 is labeled only in those afferents bearing synaptic ribbons (C). In the high magnification (D) of the OHC indicated by the arrow in C, GluK2 is colocalized with synaptic ribbons (arrows) and also labels in patches at the bottom of OHCs, corresponding to the area of efferent terminal contact (see B). (E, F, G) GluK5 is detected in OHC afferent and efferent synaptic regions. GluK5 labels in all afferent synapses (E). In the high magnification (F) of the OHC indicated by the arrow in E, GluK5 is colocalized with two afferent terminals with intense labeling (arrows) and with lower labeling at the other afferent terminals; it also labels in the area of efferent terminal contact in patches, similar to GluK2. Intense labeling of GluK5 in afferent terminals is associated with labeling for the synaptic ribbon (G, arrows). (H, I) GluK1 is detected in

OHC efferent synaptic regions only. GluK1 labeling is found in the synaptic area of OHC efferent terminals but not in afferent terminals (H). In the high magnification (I) of the OHC indicated by the arrow in H, clusters of labeling appear to be formed from several active zones in each synaptic terminal that is outlined in blue; note that blue is phalloidin in A–G and Na^+/K^+-ATPase α3 in H, I. Scale bar is 10 μm (A, B, C, E, H).

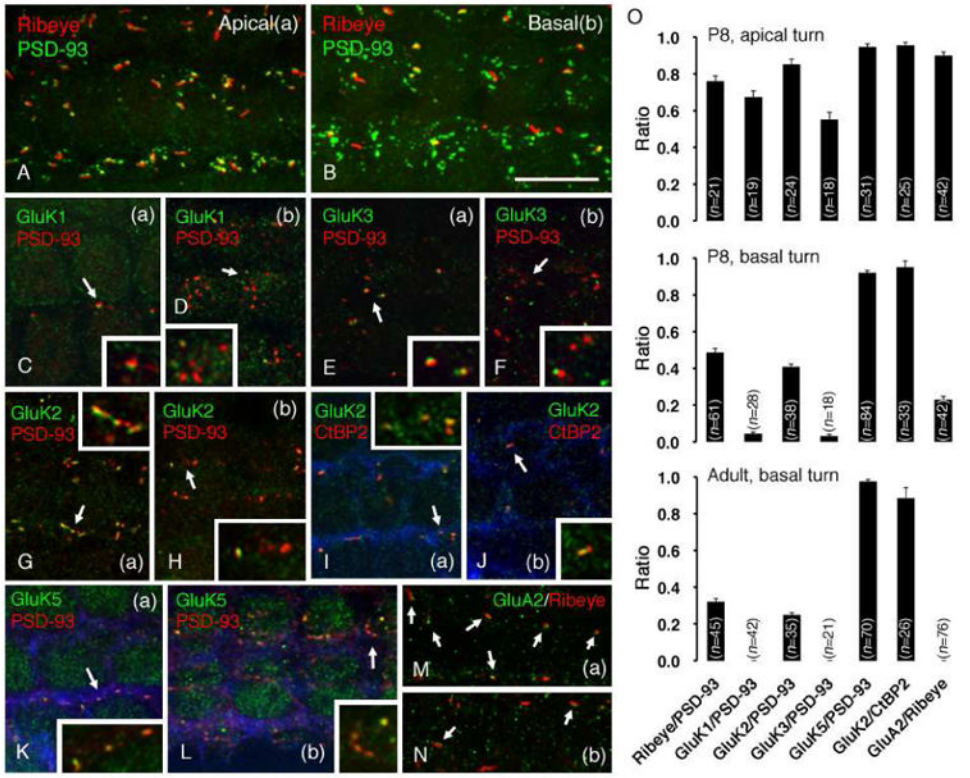

Fig. 6.

GluRs show a developmental change of expression in OHCs. The apical turn (a) and basal turn (b) of whole-mount rat cochleae at P8 were used. Afferent synapses were visualized using PSD-93 (A-H, K, L) or ribeye/CtBP2 (I, J, M, N). The strial side is on the upper side in all panels. In A and B, a maximum intensity projection of the z-stack was used to represent the entire synaptic area of each OHC. The inset in each panel shows magnification (2×) of synapses in the area in dicated by the arrow. (A, B) In the apical turn (A), there are few PSD-93-labeled terminals and each one bears a synaptic ribbon. In the basal turn (B), the number of terminals increases (increase in PSD-93-1040 labeled puncta) and the number of synaptic ribbons decreases. Consequently, few terminals are associated with synaptic ribbons, showing a pattern of expression that is similar to that seen in the adult (see Fig. 5-A). (C, D) GluK1 is expressed in afferent terminals in the apical turn (C), but is diminished in the basal turn (D). (E, F) Similar to GluK1, GluK3 is expressed in afferent terminals in the apical turn (E), but is diminished in the basal turn (F). (G, H, I, J) GluK2 is closely associated with PSD-93-labeled afferent terminals in the apical turn (G), but few terminals are labeled for GluK2 in the basal turn (H). GluK2 labeling is completely associated with labeling of synaptic ribbons in both apical (I) and basal (J) turns. Phalloidin is colored in blue to show the individual OHCs. (K, L) GluK5 is detected in each afferent terminal in both apical (K) and basal (L) turns. (M, N) GluA2 is associated with synaptic ribbons in the apical turn (M, arrows) but is barely detected in the basal turn (N, arrows). Scale bar is 10 μm. (O) Quantification of a ratio of synaptic ribbons (ribeye) or KARs to afferent synapses (PSD-93) in the apical and basal turn at P8 and basal turn in the adult. Each bar represents the mean ratio ± SEM for the indicated number of OHCs measured (n). The ratio of

synapses bearing a synaptic ribbon decreases during development. GluK1, GluK3 and GluA2 are expressed in early development but completely lost in adult. The expression pattern of GluK2 is paralleled with that of synaptic ribbons in OHC afferent synapses. On the other hand, GluK5 maintains its expression in OHC afferent synapses throughout development.